BMB
*Reports*

**BMB Rep. 2024; 57(11): 497-502**
www.bmbreports.org

# Differential roles of N- and C-terminal LIR motifs in the catalytic activity and membrane targeting of RavZ and ATG4B proteins

*Sang-Won Park[1,2], Ju-Hui Park[3], Haneul Choi[4], Pureum Jeon[4], Seung-Hwan Lee[3], Won-Dong Shin[1,2], Hun-Joo Kim[1], Jin-A Lee[4,*] & Deok-Jin Jang[1,2,3,*]*

[1]Department of Vector Entomology, College of Ecology and Environment, Kyungpook National University, Sangju 37224, [2]Research Institute of Invertebrate Vector, Kyungpook National University, Sangju 37224, [3]Department of Ecological Science, College of Ecology and Environment, Kyungpook National University, Sangju 37224, [4]Department of Biological Sciences and Biotechnology, College of Life Sciences and Nanotechnology, Hannam University, Daejeon 34054, Korea

**Mammalian ATG8 proteins (mATG8s) are essential for selective autophagy because they recruit various proteins with LC3-interacting region (LIR) motifs to autophagic membranes. The RavZ protein, secreted by *Legionella pneumophila*, and mammalian ATG4B possess functional LIR motifs that participate in lipidated mATG8 deconjugation on autophagic membranes. RavZ comprises three functional LIR motifs at the N- and C-terminal sides of its catalytic domain (CAD). This study demonstrated that LIR motifs at the N-terminal side of the CAD of RavZ are involved in autophagic membrane targeting and substrate recognition, while LIR motif at the C-terminal side facilitate autophagic membrane targeting. Our results also revealed that the C-terminal LIR motif in human ATG4B is pivotal in delipidating LC3B-phosphatidylethanolamine (PE), but it plays a minor role in pro-LC3B priming in the cytosol. Therefore, introducing a functional LIR motif to the N-terminal of ATG4B does not affect LC3B-PE delipidation. This study clearly described the position-dependent roles of LIR motifs in RavZ and ATG4B in cellular contexts. [BMB Reports 2024; 57(11): 497-502]**

## INTRODUCTION

Xenophagy is a selective autophagy process that targets intracellular pathogens, such as bacteria, viruses, and fungi, for degradation (1). Interestingly, to counteract host autophagy, many pathogens have evolved mechanisms. For example, the bacterium *Legionella pneumophila* impairs host autophagy through its effector protein, RavZ; this protein disrupts autophagosome formation by detaching mammalian autophagy-related gene 8 (mATG8) from phosphatidylethanolamine (PE) on autophagosome membranes (2, 3). It acts by cleaving the amide bond between the carboxyl-terminal glycine of mATG8 and an adjacent aromatic residue; as such, it functions similarly to the host's cysteine protease ATG4B, but it has a distinct substrate specificity. Unlike ATG4B, which cleaves soluble and membrane-bound forms of LC3/GABARAP, RavZ specifically targets only membrane-anchored versions (4).

LC3-interacting region (LIR) motifs are important for mATG8 binding (5, 6). Mammalian ATG4B possesses a functional C-terminal LIR motif, efficiently binds to all forms of mATG8s, and cleaves them in the cytosol and on membranes (7). Conversely, RavZ contains three LIR motifs: two N-terminal motifs (LIR1/2) and one C-terminal motif (LIR3). These motifs help recognize mATG8s either in the cytosol or on the autophagosome and contribute to the targeting of autophagic membranes (8). A LIR motif-deficient RavZ mutant can still non-selectively delipidate mATG8-PE without the three functional LIR motifs; as such, they play a minor role in mATG8-PE delipidation on autophagic membrane (9). However, the specific functions of each LIR motif in the targeting and enzymatic activity of RavZ remain uncertain. Recent evidence suggested that the LIR2 motif participates in the initial recognition of LC3 on autophagic membranes *in vitro* (10).

This study elucidated the differential contributions of LIR motifs at the N- and C-terminal sides of the catalytic domain (CAD) of RavZ. We found that LIR motifs at the N-terminal side of CAD primarily facilitated substrate recognition by the CAD on autophagic membranes; conversely, all LIR motifs contributed to autophagic membrane targeting. Additionally, we also confirmed that the LIR motif of ATG4B is a major factor in mATG8-PE delipidation on autophagic membranes.

*Corresponding authors. Deok-Jin Jang, Tel: +82-54-530-1213; Fax: +82-54-530-1218; E-mail: jangdj@knu.ac.kr; Jin-A Lee, Tel: +82-42-629-8785; Fax: +82-42-629-8789; E-mail: leeja@hnu.kr

https://doi.org/10.5483/BMBRep.2024-0084

**Received 27 May 2024, Revised 8 July 2024,
Accepted 2 September 2024, Published online 4 October 2024**

**Keywords:** ATG4B, Autophagy, Delipidation, Membrane localization, RavZ

ISSN: 1976-670X (electronic edition)

## RESULTS AND DISCUSSION

### Elucidating the distinct roles of LIR motifs at the N- and C-terminal sides of the CAD of RavZ

RavZ possesses three LC3-interacting region (LIR) motifs: LIR1 and LIR2 at the N-terminal and LIR3 at the C-terminal. To elucidate the roles of these LIR motifs at the N- and C-terminal sides of CAD of RavZ, we utilized deconjugase-Fy, a modified version of the protein (11). This version incorporates two identical selective LC3 subfamily-binding LIR motifs from Fyco1; thus, it replaces the native LIR1/2 and LIR3 in a 3xFLAG-tagged catalytically active but membrane-targeting (MT) domain-deficient RavZ mutant. Previous reports indicated that the expression of deconjugase-Fy selectively reduces eGFP-LC3A/B-containing autophagic membranes in rapamycin-treated hexa mATG8 knockout HeLa (HKO) cells (11). We produced eGFP-tagged deconjugase-Fy (eGFP-Fy-CAD-Fy) by replacing the 3xFLAG tag with eGFP; as a result, we formed two constructs: eGFP-Fy-CAD with a single N-terminal LIR(Fy) and eGFP-CAD-Fy with a single C-terminal LIR(Fy) (Fig. 1A). We then evaluated the formation of mRFP-LC3B- or mRFP-GABARAPL1-containing autophagosomes in these rapamycin-treated HKO cells, which co-express each construct with mRFP-LC3B or mRFP-GABARAPL1. The controls included eGFP-RavZ and eGFP. In contrast to eGFP, LIR(Fy)-containing constructs significantly delipidated mRFP-LC3B-PE from the autophagosome membrane (Fig. 1B, C); conversely, all constructs except eGFP-RavZ failed to inhibit the formation of mRFP-GABARAPL1-containing autophagosomes in rapamycin-treated HKO cells.

Among enzyme constructs, eGFP-CAD-Fy exhibited the significantly lowest enzymatic activity for delipidating membrane-anchored mRFP-LC3B; however, eGFP-Fy-CAD showed an enzymatic activity similar to that of eGFP-RavZ and eGFP-Fy-CAD-Fy (Fig.1B, C). These results suggested that the N-terminal LIR motif plays a more crucial role in enzymatic delipidation than the C-terminal LIR motif does.

The different delipidation efficiencies might be mediated by variable efficiencies in autophagic membrane localization. To test this hypothesis, we generated enzyme-deficient mutants by replacing the CADs of our constructs with catalytic mutants (C258S) that lacked enzymatic activities (Fig. 1D). Using the relative ratio of the eGFP fluorescence intensity between the autophagosome and the cytosol (A/C ratio analysis), we then assessed the localization of these enzyme-deficient mutants on the autophagic membrane. Figures 1E, F show that the LIR(Fy) motif-containing enzyme-deficient mutants co-localized with mRFP-LC3B-positive autophagosomes more effectively than eGFP alone. Notably, eGFP-Fy-CAD$_{C258S}$ and eGFP-CAD$_{C258S}$-Fy localized to mRFP-LC3B-positive autophagic membranes with a similar efficiency. However, all constructs except eGFP-RavZ$_{C258S}$ failed to localize to mRFP-GABARAPL1-positive autophagosomes; this failure was consistent with the known preference of LIR(Fy) for mATG8 proteins. These results demonstrated that N- and C-terminal LIR motifs contribute equally to autophagosome membrane localization; conversely, the

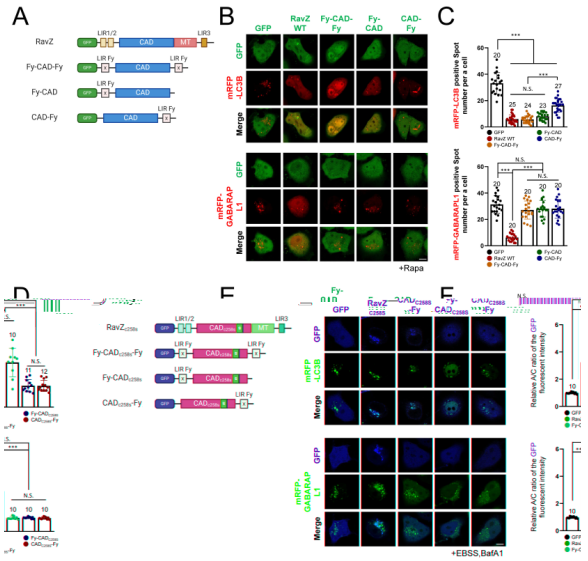


**Fig. 1.** Elucidation of different roles of LIR motifs of the modified RavZ protein using LIR(Fy). (A) Schematic of the generation of eGFP-tagged deconjugase-Fy and its LIR motif-deficient mutants. (B) Confocal images showing the autophagosome formation of mRFP-LC3B (upper) or mRFP-GABARAPL1 (lower) protein co-expressed with RavZ proteins (RavZ, wild type) or deconjugase-Fy mutants in HKO cells upon autophagy induction (100 nM rapamycin [Rapa], 4 h). Scale bar: 10 μm. (C) Bar graphs illustrating the autophagosome spot number for each cell. Values are presented as means + SEM. *** P < 0.001, one-way ANOVA with the Newman–Keuls multiple comparison test. N.S., not significant. (D) Schematic of the generation of eGFP-tagged enzyme-deficient mutant (C258S) of deconjugase-Fy and its LIR motif-deficient mutants. (E) Confocal images showing the cellular localization of RavZ$_{C258S}$ or enzyme-deficient mutants containing one or more LIR(Fy) co-expressed with mRFP-LC3B (upper) or mRFP-GABARAPL1 (lower) protein in HKO cells upon autophagy induction (100 nM bafilomycin A1 (BafA1) in Earle's balanced salt solution (EBSS) for 2 h, +EBSS, BafA1). Scale bar: 10 μm. (F) Bar graphs illustrating the quantification of the autophagosome and cytosol (A:C) ratio of GFP fluorescence in each cell. Values are presented as means + SEM . ***P < 0.001, one-way ANOVA with the Newman–Keuls multiple comparison test. N.S., not significant. The numbers above the bar graph represent the number of replicates for each experiment.

N-terminal LIR motif plays a more remarkable role than the C-terminal LIR motif in the delipidation of membrane-anchored LC3B on autophagic membranes.

To further clarify the distinct roles of N- and C-terminal LIR motifs, we utilized two LIR motifs with different selective mATG8 binding properties: LIR(Fy) for LC3B and LIR(St) for GABARAPL1. We created the following constructs: eGFP-Fy-CAD-St, which incorporates N-terminal LIR motifs from Fyco1 and C-terminal from Stbd1; and eGFP-St-CAD-Fy, which has the N-terminal motif from Stbd1 and the C-terminal from Fyco1 (Fig. 2A). eGFP-Fy-CAD-St overexpression completely eliminated mRFP-LC3B-containing autophagosomes and partially reduced mRFP-GABARAPL1-containing autophagosomes, unlike cells

that expressed only eGFP-CAD (Fig. 2B, C). Conversely, eGFP-St-CAD-Fy completely disrupted mRFP-GABARAPL1-containing autophagosomes and slightly affected mRFP-LC3B-containing ones (Fig. 2B, C). These findings emphasized that the effect of the N-terminal LIR motif on the delipidation of membrane-anchored LC3B within autophagic membranes is more considerable than that of the C-terminal motif.

To determine and confirm the importance of the order and presence of different LIR motifs when positioned consecutively at the N-terminus or C-terminus, we created constructs such as eGFP-Fy-St-CAD, eGFP-St-Fy-CAD, eGFP-CAD-Fy-St and eGFP-CAD-St-Fy, which alternated the order of LIR motifs for LC3B and GABARAP. The overexpression of eGFP-Fy-St-CAD and eGFP-St-Fy-CAD efficiently and completely eliminated the formation of mRFP-LC3B- and mRFP-GABARAPL1-containing autophagosomes. Conversely, overexpression of eGFP-CAD-Fy-St and eGFP-CAD-St-Fy less efficiently eliminate mRFP-LC3B- and mRFP-GABARAPL1-positive autophagosomes compared to eGFP-Fy-St-CAD and eGFP-St-Fy-CAD (Fig. 2B, C). These findings indicated that while the presence of the LIR motifs at the N-terminus is crucial for mATG8-PE delipidation, the sequence of these motifs at the N-terminus does not substantially affect their catalytic function.

Overall, our findings indicated that the N- and C-terminal LIR motifs of RavZ contribute similarly to autophagic membrane localization. However, in the context of autophagosomes, the N-terminal LIR motif is more important than the C-terminal LIR motif for substrate recognition.

## Elucidating the roles of a LIR motif in human ATG4B for the priming and delipidation of overexpressed LC3B in ATG4B knockout HeLa Cells

The mammalian ATG4 family proteins, which are cysteine protease that cleaves the C-terminal of LC3/GABARAP proteins, consists of 4 different members (ATG4A, B, C, and D) and have a dual function priming LC3/GABARAP lipidation and delipidation in the autophagy pathway (12). Especially, ATG4B effectively mediates both the priming and delipidation of all LC3/GABARAP proteins (13, 14). ATG4B contains a single functional LIR motif at its C-terminal end, which binds to all types of LC3/GABARAP proteins (7). To directly examine the priming of LC3/GABARAP proteins by ATG4B in cells via confocal microscopy, we prepared a MyrPalm-LC3B[G-M]eGFP construct. In this construct, starting with methionine, eGFP is directly linked to the glycine residue at the end of the LC3B protein. The MyrPalm motif is a short amino acid sequence "GCCNSKRKD" that localizes to the plasma membrane through myristoylation and palmitoylation (15). It artificially targets MyrPalm-LC3B[G-M]eGFP to plasma membranes (Fig. 3A). To evaluate the cleavage of LC3B from eGFP by endogenous ATG4B, we expressed MyrPalm-LC3B[G-M]eGFP in

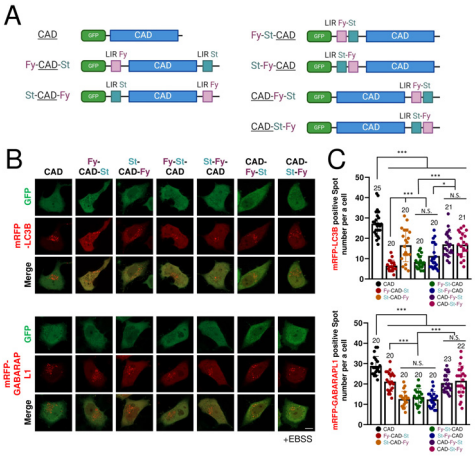


**Fig. 2.** Elucidation of the different roles of LIR motifs of the modified RavZ protein using different LIR motifs. (A) Schematic of the generation of chimeric mutants containing LIR(Fy) and LIR(St) with different binding specificities. (B) Confocal images showing the autophagosome formation of mRFP-LC3B (upper) or mRFP-GABARAPL1 (lower) protein co-expressed with chimeric mutants in HKO cells upon autophagy induction (Earle's balanced salt solution [EBSS] for 2 h). Scale bar: 10 μm. (C) Bar graphs illustrating the autophagosome spot number for each cell. Values are presented as means + SEM . *** $P < 0.001$, one-way ANOVA with the Newman–Keuls multiple comparison test. N.S., not significant. The numbers above the bar graph represent the number of replicates for each experiment.

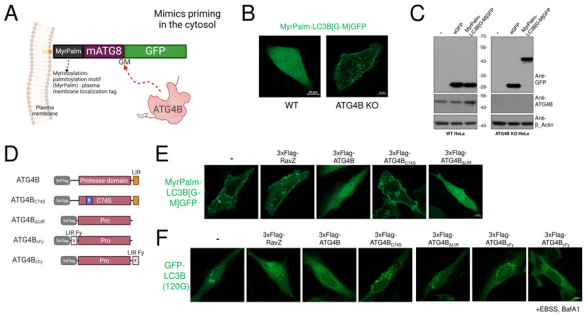


**Fig. 3.** Elucidation of the roles of LIR motifs of ATG4B. (A) Schematic of MyrPalm-mATG8-eGFP constructs and the "priming" of pro-LC3/GABARAP into an LC3/GABARAP-1 form. MyrPalm, myristoylation, and palmitoylation motif. (B) Confocal images showing the cellular localization of MyrPalm-LC3B[G-M]eGFP in WT HeLa and ATG4B KO HeLa cells. Scale bar: 10 μm. (C) Representative western blots of overexpressed MyrPalm-LC3[G-M]eGFP proteins in WT HeLa and ATG4B KO HeLa cells with the indicated anti-GFP, anti-ATG4B, and anti-β-actin antibodies. (D) Schematic of several 3xFlag-fused ATG4B and variants. ATG4B$_{C74S}$, catalytically inactive mutant; Fy, LIR motif of Fyco1; Pro, protease domain. (E) Confocal images showing the cellular localization of MyrPalm-LC3B[G-M]eGFP co-expressed with RavZ, ATG4B, ATG4B$_{C74S}$, and LIR-deletion mutant (ATG4B$_{\triangle LIR}$) in ATG4B KO HeLa cells. (F) Confocal images showing the autophagosome formation of eGFP-LC3B (120G) co-expressed with RavZ, ATG4B, and all variants with protease domains in ATG4B KO HeLa cells upon autophagy induction (100 nM bafilomycin A1 [BafA1] in Earle's balanced salt solution [EBSS] for 2 h, +EBSS, BafA1).

wild-type and ATG4B knockout (KO) HeLa cells. We observed eGFP-expressing cells under a confocal microscope and conducted western blot analysis by using an anti-GFP antibody. When MyrPalm-LC3B[G-M]eGFP was overexpressed in wild-type HeLa cells, eGFP was cleaved by ATG4B at the terminal glycine of the overexpressed LC3B and released diffusely into the cytosol and nucleus within 24 h after transfection. In ATG4B KO HeLa cells, MyrPalm-LC3B[G-M]eGFP remained localized to the plasma membrane because of the MyrPalm motif; this result indicated that LC3B[G-M]GFP was not cleaved. Western blot analysis revealed a small cleaved eGFP band in wild-type HeLa cells but not in ATG4B KO HeLa cells. Therefore, this result confirmed that ATG4B cleaves eGFP from the C-terminal of LC3B proteins in cells (Fig. 3B, C).

To investigate the role and importance of the LIR motif of ATG4B in the priming and delipidation of LC3/GABARAP proteins, we created 3xFLAG-ATG4B$_{\triangle LIR}$, a mutant that lacks the C-terminal LIR motif (Fig. 3D). We co-expressed this mutant with MyrPalm-LC3B[G-M]eGFP in ATG4B knockout (KO) HeLa cells and assessed eGFP localization 24 h post-transfection. The exogenously expressed 3xFLAG-ATG4B and 3xFLAG-ATG4B$_{\triangle LIR}$ proteins, not the catalytically inactive 3xFLAG-ATG4B$_{C74S}$ mutant, successfully cleaved eGFP from LC3B at the plasma membrane (Fig. 3E). Conversely, RavZ did not cleave eGFP from LC3B. Although our experimental setup did not completely rule out the contribution of the LIR motif to early "priming" because of the 24 h post-transfection analysis, we demonstrated that the protease CAD of ATG4B alone is adequate for the "priming" of LC3B proteins under our experimental conditions. Conversely, RavZ failed to prime LC3B proteins. This result was consistent with previous finding (2).

To assess the role of the LIR motif of ATG4B in the delipidation of LC3B-PE on autophagosomes, we constructed an eGFP-LC3B (120G) truncation that ended with a glycine residue (pre-primed form), consequently bypassing the need for priming. The overexpression of 3xFLAG-ATG4B and 3xFLAG-RavZ notably reduced the formation of eGFP-LC3B-containing autophagosomes in ATG4B KO HeLa cells during autophagy induction and inhibition with 100 nM bafilomycin A1 (BafA1) in Earle's balanced salt solution (EBSS) for 2 h (Fig. 3F). Conversely, the overexpression of the catalytically inactive 3xFLAG-ATG4B$_{C74S}$ did not reduce the formation of eGFP-LC3B-containing autophagosomes. Interestingly, the 3xFLAG-ATG4B$_{\triangle LIR}$ overexpression led to the formation of eGFP-LC3B-containing autophagosomes at levels comparable with those observed in 3xFLAG-ATG4B$_{C74S}$ under the same conditions. These findings demonstrated that the C-terminal LIR motif of ATG4B is critical for LC3B-PE delipidation from the autophagosome membrane.

The LIR motif localized at the N-terminal of RavZ is more crucial for the delipidation of mATG8-PE on the autophagic membrane (Fig. 1 and 2). To further explore the role of the LIR motif, we incorporated either N- or C-terminal LIR(Fy) motifs into 3xFLAG-ATG4B$_{\triangle LIR}$; thus, we created 3xFLAG-ATG4B$_{nFy}$ and 3xFLAG-ATG4B$_{cFy}$. Furthermore, 3xFLAG-ATG4B$_{cFy}$, not

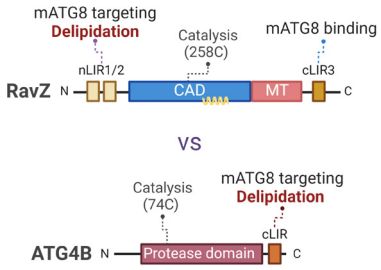


**Fig. 4.** Elucidation of the role of each LIR motif in RavZ vs. ATG4B. Schematic of the function and mechanism of action of the respective domains and LIR motifs of RavZ and ATG4B proteins. The N-terminal LIR of RavZ is important for interaction with mATG8-PE and for the catalytic activity of CAD, while the C-terminal LIR is essential for maintaining the binding to mATG8-PE in the autophagic membrane. The C-terminal LIR of ATG4B interacts with mATG8 and cleaves the termini of various forms (pro-mATG8 or mATG8-II) of mATG8 proteins in the cytosol (priming) and at the autophagic membrane (delipidation).

3xFLAG-ATG4B$_{cFy}$, reduced the formation of eGFP-LC3B-positive autophagosomes (Fig. 3F). In contrast to RavZ, the C-terminally localized LIR motif plays an important role in LC3B-PE delipidation on autophagosomes.

In the case of RavZ, the catalytic domain of RavZ has membrane association properties but lacks direct LC3 binding capability. Therefore, the LIR motif of RavZ is necessary for the initial recognition of mATG8s on the autophagic membrane (4, 10). The catalytic domain then extracts the PE moiety of mATG8-PE from the autophagic membrane and deconjugates it while binding to the acyl chain of PE (10). Consequently, the LIR motif located at the N-terminus relative to the membrane-bound catalytic domain is crucial for supporting the subsequent processing by the catalytic domain.

In contrast, the catalytic domain of ATG4B can directly bind to mATG8s (7), which is why it can prime pro-LC3B to LC3B-I independently. However, the catalytic domain alone cannot delipidate lipidated LC3B on the autophagic membrane. Given that ATG4B deconjugates LC3B-PE without extraction, an additional motif is required to enable the catalytic domain to access lipidated LC3B on the autophagic membrane. Interestingly, the C-terminal LIR motif of ATG4B wraps around the LC3B core domain, which is already occupied by the catalytic domain, thereby enhancing the binding strength between ATG4B and LC3B (16). Therefore, unlike the classical binding of the LIR motif to the LC3B core, the C-terminal LIR motif of ATG4B binds to pre-occupied LC3B in an atypical manner.

On the basis of our current study, we proposed that the N- and C-terminal LIR motifs in RavZ had different roles (Fig. 4). RavZ targets autophagosome membranes through multiple pathways: an membrane targeting (MT) domain via PI3P/PI(3,5)$P_2$ binding, the α3 motif in the catalytic domain via membrane association, and the N- and C-terminal LIR motifs via mATG8 binding. Initially, RavZ proteins delipidate tethered mATG8s predominantly via N-terminal LIR motifs, including LIR1 and

LIR2. However, the contribution of LIR1 and 2 motifs to tethered mATG8 delipidation by N-terminal LIR motifs is negligible, as demonstrated by the lack of differences between 3xFLAG-RavZ($\triangle$MT)$_{mLIR3}$ and 3xFLAG-RavZ($\triangle$MT)$_{C258S}$(9). Indeed, RavZ can be stably localized to the autophagic membrane through an MT domain or the C-terminal LIR motif, in addition to the $\alpha$3 motif in the CAD; thus, it can non-selectively delipidate nearby mATG8s-PE. For ATG4B, the protease CAD alone is sufficient for the "priming" of pro-LC3B into the LC3B-I form (Fig. 3E). This finding is consistent with reports that the CAD of ATG4B can bind to LC3B (7), indicating that this interaction is sufficient for cleaving pro-LC3B in a solution. Additionally, the C-terminal LIR motif on the autophagic membrane participates in LC3B-PE delipidation by ATG4B (Fig. 3F).

Our study showed the importance of LIR motif positioning in the functionality of proteins such as RavZ and ATG4B in the autophagy pathway. For RavZ, N-terminal LIR motifs participate in delipidation; for ATG4B, the C-terminal LIR motif is essential for delipidating LC3B-PE on autophagosomes (Fig. 4). The LIR motif has traditionally been considered non-essential in terms of its position within the protein, as it functions by binding to specific mATG8s to facilitate targeting. However, our study reveals that the function of the LIR motif can vary depending on its relative position within the protein, influenced by the structure and mechanism of the catalytic domain. Therefore, it is crucial to consider not only which mATG8s the LIR motif binds to but also its position within the protein. Additionally, based on our findings, we propose that introducing various combinations of LIR motifs at the N- or C-terminus of RavZ or ATG4B could lead to the development of recombinant proteins with distinct regulatory effects on various autophagic pathways. Our results challenge the prevailing assumptions about the redundancy of LIR motifs in such proteins and offer new insights into their functional specialization and interaction dynamics with autophagic membranes. This understanding of LIR motif roles clarifies their contribution to autophagy. It also provides a basis for establishing potential therapeutic strategies that target these pathways in diseases associated with autophagy dysregulation.

## MATERIALS AND METHODS

### DNA constructs

All primer sequences used in these experiments are listed in Supplemental Table 1. eGFP-tagged deconjugase-Fy and enzyme-deficient mutant form (C258S) of deconjugase-Fy were constructed by replacing the existing 3xFlag tag with PCR-amplified eGFP. The amplified eGFP was inserted into C1-deconjugase-Fy and C1-deconjugase-Fy(C258S) vectors by using a specific set of restriction enzymes (Nhe1-BglII; R016S and R010S, Enzynomics, Daejeon, Korea). The LIR deletion mutant forms were amplified with their respective primer sets and inserted into the C1-eGFP vector with the specific restriction enzymes (EcoR1-Apa1; R002S and R020S, Enzynomics, Daejeon, Korea). Each LIR was amplified through PCR and inserted into the C1-eGFP-CAD vector via restriction enzymes (BglII or SalI; R010S and R009S, Enzynomics, Daejeon, Korea) to create chimeric mutants containing LIR(Fy) and LIR(St). ATG4B and ATG4B$_{C74S}$ were obtained from Addgene (#190862, Addgene, Watertown, MA). The LIR deletion mutant of ATG4B and the LIR(Fy)-containing ATG4B constructs were also amplified with their respective primer sets and inserted into C1-3xFLAG-ATG4B or C1-3xFLAG-deconjugase-Fy vectors by using Gibson Assembly® Master Mix (E2611, New England Biolabs, Ipswich, MA). MyrPalm, LC3B[120G], and eGFP were each amplified via PCR and ligated into pcDNA3.1(+) vector by using Gibson Assembly® Master Mix to create the MyrPalm-LC3B[G-M]eGFP construct. Previously described DNA constructs for mRFP-LC3B, mRFP-GABARAPL1, RavZ, RavZ$_{C258S}$, and deconjugase-Fy were used in this study.

### Cell culture and transfection

Human ATG4B knockout HeLa cell line was purchased from Abcam (ab265814, Abcam, Cambridge, UK). HeLa cells and ATG4B knockout HeLa cells were cultured in Dulbecco's modified Eagle's medium (DMEM; 11965092, Thermo Fisher Scientific, Waltham, MA) and supplemented with 10% (v/v) fetal bovine serum (FBS; 12483020, Thermo Fisher Scientific, Waltham, MA) and penicillin/streptomycin (15140122, Thermo Fisher Scientific, Waltham, MA) in a humidified atmosphere with 5% (v/v) $CO_2$ at 37°C. mATG8 HKO HeLa cells were cultured in DMEM and supplemented with 15% (v/v) FBS and penicillin/streptomycin in a humidified atmosphere with 5% (v/v) $CO_2$ at 37°C. The cells were seeded in a sticky-slide eight-well system (#80828, Ibidi, Martinsried, Germany) to obtain 40%-60% confluent cells on the day of imaging. They were transfected with the indicated DNA constructs by using calcium phosphate or Lipofectamine 2000 (631312, Takara bio, Kusatsu, Japan and 11668500, Invitrogen, Waltham, MA) 24-26 h before imaging. The relative amount of each construct was empirically calculated in terms of the relative expression of each construct combination.

### Confocal microscopy and drug treatment

Cells were observed using an inverted Zeiss LSM-900 scanning laser confocal microscope with ZEN software (Carl Zeiss, Oberkochen, Germany). The laser lines for excitation and the spectral detection windows for fluorochromes were 488 nm (508-543 nm for eGFP) and 561 nm (578-649 nm for mRFP), respectively. Each fluorescent protein was sequentially imaged using appropriate eGFP (500-550 nm) and mRFP (575-625 nm) emission filters Most of the images have been taken from living cells.

Rapamycin (Rapa) was obtained from Sigma-Aldrich (553210, Sigma-Aldrich, St. Louis, MO). Cells were incubated with 100 nM rapamycin in DMEM + 10 or 15% FBS for 2-4 h to induce autophagy. All treatments and assays were performed at 37°C unless otherwise indicated. Autophagy-deficient cells were treated with 100 nM bafilomycin $A_1$ (B1793, Sigma-Aldrich, St. Louis, MO) in EBSS (E3024, Sigma-Aldrich, St. Louis, MO) for 2 h to accumulate autophagosomes.

### Western blot analysis

Transfected HeLa or ATG4B KO HeLa cell lysates were prepared by adding cells to a lysis buffer solution (50 mM Tris, pH 7.5, 150 mM NaCl, 0.5% sodium deoxycholate, 0.2% SDS, 0.2% NP-40, and protease inhibitors). Equal amounts of protein were resolved by SDS-PAGE, transferred to PVDF membranes, and incubated with primary antibodies at 4°C overnight. After being washed thrice, the membranes were incubated with secondary antibodies conjugated with horseradish peroxidase for 1 h. Signals were visualized with a Western Bright ECL kit (K-12045-D50, Advansta, San Jose, CA). The following antibodies were used: eGFP antibody (sc-9996, Santa Cruz Biotechnology, Dallas, TX) at 1:10,000, LC3 antibody (#2775, Cell Signaling Technology, Danvers, MA) at 1:1000, β-actin antibody (sc-47778, Snta Cruz Biotechnology, Dallas, TX) at 1:1000, and ATG4B antibody (ab154843, Abcam, Cambridge, UK). The following secondary antibodies were used: HRP-conjugated mouse anti-rabbit (1:10,000; sc-2357, Santa Cruz Biotechnology, Dallas, TX) and HRP-conjugated mouse IgG kappa binding protein (1:10,000; sc-516102, Santa Cruz Biotechnology, Dallas, TX).

### Counting of LC3/GABARAP-positive autophagosomes (spot number analysis)

The number of spots over a certain field size in a single cell was counted using the ImageJ software to determine the reduction in LC3/GABARAP-positive autophagosomes through the enzyme activation of RavZ in autophagy-induced cells. The cell image was changed to an 8-bit image and inverted. Then, the background was removed so that only the spot remained visible. The number of spots was counted using the "Analyze particles" function of Image-J. A minimum of 20 cells was quantified using this approach. Statistical data were calculated and graphed using GraphPad Prism8 (GraphPad, La Jolla, CA).

### Quantitative analysis of autophagosome/cytosol (A/C) fluorescent intensities

The average value of the vesicle or cytosol fluorescent intensity was obtained from at least five randomly selected points on the vesicles or in the cytosol of a single cell by using the ZEN software to calculate the ratio of autophagosome/cytosol (A/C) fluorescent intensities. Similarly, the quantitative A/C ratio of at least 10 randomly selected cells per experiment was determined from three independent experiments. Statistical data were calculated and graphed using GraphPad Prism8 (GraphPad, La Jolla, CA).

## ACKNOWLEDGMENTS

The work was supported by the Science Research Center Program of the National Research Foundation NRF (2020R1A5A1019023); Neurological Disorder Research Program of the NRF (2020M3E5D9079911); Basic research program of the NRF (2023R1A2C2008092) to JAL. D.-J.J. was supported by the Basic Research Program of NRF (2022R1F1A1066552), and the NRF grant funded by the Korea government (MSIT) (RS-2023-00218515).

## CONFLICTS OF INTEREST

The authors have no conflicting interests.

## REFERENCES

1. Kwon DH and Song HK (2018) A Structural view of xenophagy, a battle between host and microbes. Mol Cells 41, 27-34
2. Choy A, Dancourt J, Mugo B et al (2012) The Legionella effector RavZ inhibits host autophagy through irreversible Atg8 deconjugation. Science 338, 1072-1076
3. Horenkamp FA, Kauffman KJ, Kohler LJ et al (2015) The legionella anti-autophagy effector ravz targets the autophagosome via PI3P- and curvature-sensing motifs. Dev Cell 34, 569-576
4. Maruyama T and Noda NN (2017) Autophagy-regulating protease Atg4: structure, function, regulation and inhibition. J Antibiot (Tokyo) 71, 72-78
5. Birgisdottir Å B, Lamark T and Johansen T (2013) The LIR motif - crucial for selective autophagy. J Cell Sci 126, 3237-3247
6. Rogov VV, Nezis IP, Tsapras P et al (2023) Atg8 family proteins, LIR/AIM motifs and other interaction modes. Autophagy Rep 2, 27694127
7. Skytte Rasmussen M, Mouilleron S, Kumar Shrestha B et al (2017) ATG4B contains a C-terminal LIR motif important for binding and efficient cleavage of mammalian orthologs of yeast Atg8. Autophagy 13, 834-853
8. Kwon DH, Kim S, Jung YO et al (2017) The 1:2 complex between RavZ and LC3 reveals a mechanism for deconjugation of LC3 on the phagophore membrane. Autophagy 13, 70-81
9. Park SW, Jun YW, Jeon P et al (2019) LIR motifs and the membrane-targeting domain are complementary in the function of RavZ. BMB Rep 52, 700-705
10. Yang A, Pantoom S and Wu YW (2017) Elucidation of the anti-autophagy mechanism of the Legionella effector RavZ using semisynthetic LC3 proteins. Elife 6, e23905
11. Park SW, Jeon P, Yamasaki A et al (2023) Development of new tools to study membrane-anchored mammalian Atg8 proteins. Autophagy 19, 1424-1443
12. Agrotis A, Pengo N, Burden JJ and Ketteler R (2019) Redundancy of human ATG4 protease isoforms in autophagy and LC3/GABARAP processing revealed in cells. Autophagy 15, 976-997
13. Tanida I, Sou YS, Ezaki J, Minematsu-Ikeguchi N, Ueno T and Kominami E (2004) HsAtg4B/HsApg4B/autophagin-1 cleaves the carboxyl termini of three human Atg8 homologues and delipidates microtubule-associated protein light chain 3- and GABAA receptor-associated protein-phospholipid conjugates. J Biol Chem 279, 36268-36276
14. Nakatogawa H, Ishii J, Asai E and Ohsumi Y (2012) Atg4 recycles inappropriately lipidated Atg8 to promote autophagosome biogenesis. Autophagy 8, 177-186
15. Osteikoetxea X, Silva A, Lázaro-Ibáñez E et al (2022) Engineered Cas9 extracellular vesicles as a novel gene editing tool. J Extracell Vesicles 11, e12225
16. Tang Y, Kay A, Jiang Z and Arkin MR (2022) LC3B binds to the autophagy protease ATG4b with high affinity using a bipartite interface. Biochemistry 61, 2295-2302